Highly sensitive NADH detection by utilising an aluminium hydroxide/iron hydroxide/MWCNTs nanocomposite film-modified electrode

Yu Wang[1], Lingling Yin[2], Xia Li[1], Ran Shang[1], Xiangli Yang[1], Xiaoyan Zhou[1], Yen Chen[1] ✉

[1]*School of Resources and Environmental Engineering, Shandong Agriculture and Engineering University, Jinan, 250100, People's Republic of China*
[2]*Shandong Provincial Veterinary Medicine Supervision Institute/Shandong Provincial Key Laboratory of Quality Safety Monitoring and Risk Assessment for Livestock and Poultry Products, Jinan, 250022, People's Republic of China*
✉ *E-mail: ychen0612@163.com*

Published in Micro & Nano Letters; Received on 6th February 2020; Revised on 29th May 2020; Accepted on 3rd August 2020

Glassy carbon electrode (GCE) modified with aluminium hydroxide/iron hydroxide/multi-walled carbon nanotubes (AH/IH/MWCNTs) composites has been prepared by a simple method and applied for dihydro-nicotinamide adenine dinucleotide (NADH) detection. AH/IH can not only accelerate electron transfer but also electrostatically interact with the phosphate groups of NADH through iron hydroxide to improve the sensitivity of the sensor. Meanwhile, MWCNTs served as a bonding agent to provide a built-in conductor, which resulted in boosted electron transfer at the interface. Compared with the GCE, MWCNTs–GCE, and AH/MWCNTs–GCE, the AH/IH/MWCNTs–GCE exhibited an extraordinary electrocatalytic response towards NADH, with a wide linear concentration range from 0.5 to 220 μM with a low-detection limit of 0.30 μM, at a comparatively low potential (+0.15 V versus Ag/AgCl). Moreover, alcohol dehydrogenase was used as a model system for the design of a sensitive ethanol biosensor. The resulting biosensor exhibited an ethanol sensitivity of 9 μA/mM, a concentration range of 20–400 μM, and a detection limit of 5 μM. These results demonstrate the potential of the AH/IH/MWCNTs nanocomposite film for biosensors in combination with NADH-producing enzymes.

1. Introduction: Dihydronicotinamide adenine dinucleotide (NADH) plays an important role in the electron transport chain inside cells [1, 2]. Besides, NADH is associated with diseases such as cancer, depression, Parkinson's and Alzheimer's [3]. Hence, in the fields of biotechnology and molecular diagnostics, developing sensitive and selective methods for fast and accurate monitoring of NADH has gained extensive attention. Many techniques have been used for NADH determination, including spectroscopy, chromatography, capillary electrophoresis, electrochemistry, and enzymatic assays [2, 4–7]. Among these, electrochemical methods have been widely employed to determinate NADH due to their high selectivity, sensitivity, fast detection, economic efficiency, and easy preparation [8–10]. Nevertheless, at conventional electrodes, NADH oxidation usually takes place at high overpotential, which results in the surface passivation and fouling [11, 12]. Modification of the electrode has been suggested as a way to low the overpotential and allow NADH oxidation to be easily realised [10, 13–15]. Redox mediators, nanotubes, inorganic nanoparticles, and conducting polymers are frequently used for modifiers to promote electron transfer between NADH and the electrode. They significantly reduced the oxidation overpotential, promote the electron transfer rate and enhance the anti-fouling ability of the electrode, but to a limited extent [16].

In recent years, multi-walled carbon nanotube (MWCNT)-based nanocomposites—with polymers, biomolecules, or metal or inorganic nanoparticles or ionic liquid—have been widely utilised for amperometric sensing of NADH because of the synergistic effect [9, 13, 17–20]. Recent research studies demonstrate that iron hydroxide [$Fe(OH)_3$] nanoparticles/carbon nanotube (CNT) composites have the potential for application in modified electrodes [21, 22]. $Fe(OH)_3$ nanoparticles have redox properties similar to those of frequently used mediators and the function to shuttle electrons between NADH and electrode, and they have been used in mediatorless electrochemical systems. However, shedding from the electrode surface and particle aggregation occurs during catalyst processes due to the van der Waals forces and high-surface energy between the $Fe(OH)_3$ nanoparticles [23], which limits their electrocatalysis activity. Recent studies show that as adsorbent supports, aluminium hydroxide with a hierarchical structure is uniquely advantageous to serve as a catalyst support to uniformly anchor $Fe(OH)_3$ colloid nanoparticles with well-defined size and shapes [24], and as electrically conductive adhesives, MWCNTs could prevent abscission of particles.

In this investigation, well-dispersed $Fe(OH)_3$ nanoparticles were synthesised by using monodispersed aluminium hydroxide supports with a hierarchical structure [23]. To prevent modifiers dropping from the electrode surface and enhance the electron transfer between the electrode surface and NADH, aluminium hydroxide/iron hydroxide/MWCNTs (AH/IH/MWCNTs) nanocomposites were then synthesised for sensing NADH, with low potential and low-detection limit, highly sensitive and selective. Additionally, a novel ethanol biosensor was fabricated using alcohol dehydrogenase (ADH) immobilised on the electrode surface previously modified with AH/IH/MWCNTs nanocomposite.

2. Experimental

2.1. Principal materials: The aluminium hydroxide/iron hydroxide nanocomposites were synthesised as reported in [23, 24]. Nicotinamide adenine dinucleotide (NAD^+), NADH, ADH (EC 1.1.1.1) from *Saccharomyces cerevisiae* were obtained from Sigma-Aldrich. CNTs (diameter 40–60 nm; length <2 μm; purity >97%) were obtained from Shenzhen Nanotech Port (China). A 0.1 M phosphate-buffered saline (PBS; pH 7.4) was used as the supporting electrolyte solution. All other chemicals and reagents were of analytical grade and the solutions were prepared with ultrapure water.

2.2. Electrochemical detection and characterisation: The surface morphology was observed on a Supra 55 field-emission scanning electron microscope. All electrochemical experiments were performed with a 660E electrochemical workstation (CH Instruments, Chenhua, China) with a three-electrode system that consisted of a bare or modified glassy carbon electrode (GCE; 3 mm diameter), a platinum wire, and Ag/AgCl

(3 M KCl). The oxidation behaviours of NADH on AH/IH/MWCNTs–GCE were studied by cyclic voltammetry (CV). Before each CV measurement, the electrode was placed in 5 ml PBS, and the potential scan was performed between−100 and 600 mV until a steady voltammogram was obtained. Amperometric measurements were carried out with a modified electrode in PBS while stirring (500 rpm) at a low potential (0.15 V).

2.3. Preparation of AH/IH/MWCNTs nanocomposite-modified GCEs: AH/IH nanocomposites were prepared with a hierarchical structure as previously described [23]. Prior to modification, the GCE was polished with 0.3 and 0.05 µm alumina slurries and then washed with ultrapure water. For the preparation of the electrochemical sensor, the AH/IH/MWCNTs' nanocomposites were synthesised by a self-assembly approach. Various amounts of AH/IH nanocomposites were dissolved along with 10 mg of MWCNTs in 5 ml of distilled water and subjected for 1 h to ultrasonic waves, then 5 µl of the proposed aqueous dispersion (1 mg/ml) was cast on a GCE and air-dried at room temperature. Electrodes modified with only MWCNTs or AH/MWCNTs were also prepared, by casting equal quantities of the respective solutions onto GCEs. Finally, the resulting modified electrodes were rinsed with PBS to remove unadsorbed materials.

3. Results and discussion

3.1. Characterisation of the modified electrodes: The morphology and microstructure of the surface of the modified electrodes were investigated by SEM. Figs. 1*a*–*c*, respectively, show the SEM images of the GCEs modified with MWCNTs, AH/MWCNTs, and AH/IH/MWCNTs. In MWCNTs–GCE, the MWCNTs were randomly distributed on the GCE surface because of π–π stacking and van der Waals interaction (Fig. 1*a*). In the SEM image of AH/MWCNTs–GCE (Fig. 1*b*), the MWCNTs just randomly penetrating the spacing in the film, indicating that the composite has not been formed. As displayed in Fig. 1*c*, the MWCNTs uniformly and closely attached to the surface of AH/IH as well as penetrating the spacing in the film. This indicates that agglomeration is no longer an issue and AH/IH/MWCNTs' composites have been successfully obtained on the electrode surface.

3.2. Electrochemical characterisation of the proposed electrode: The charge transfer property and effective surface area for the proposed electrodes were determined from CV measurements of 1 mM $K_4[Fe(CN)_6]$ containing 0.1 M KCl at 50 mV/s (Fig. 2). The potentials of the $K_4[Fe(CN)_6]$ redox peaks were similar among the proposed electrodes. The current of AH/IH/MWCNTs–GCE was significantly higher than that of the other electrodes, indicating that $Fe(OH)_3$ played an important role in the increase of the electronic transport capacity of the electrode. Additionally, to further characterise the surface features of the modified electrode, the specific surface area of the electrodes can be found by the Randles–Sevcik equation [25]

$$I_p = 2.69 \times 10^5 A D^{1/2} n^{3/2} v^{1/2} C \quad (1)$$

where A is the specific surface area (cm^2), I_p is the peak current value, and D is the diffusion coefficient of $K_4[Fe(CN)_6]$ (the value is 6.7×10^{-6} cm^2/s under 25°C), n is the transferred electron number during the reaction, v represents the scanning rate (V/s), and C is the concentration of $K_4[Fe(CN)_6]$ (mol/cm^3).

According to the above formula, the specific surface areas were calculated to be 0.017, 0.025, 0.037, and 0.069 cm^2 for bare GCE, MWCNTs–GCE, AH/MWCNTs–GCE, and AH/IH/MWCNTs–GCE, respectively. This demonstrates that the active surface area of the electrode could be improved by modification with AH with a hierarchical structure and that it could be expanded further by the adsorption of $Fe(OH)_3$.

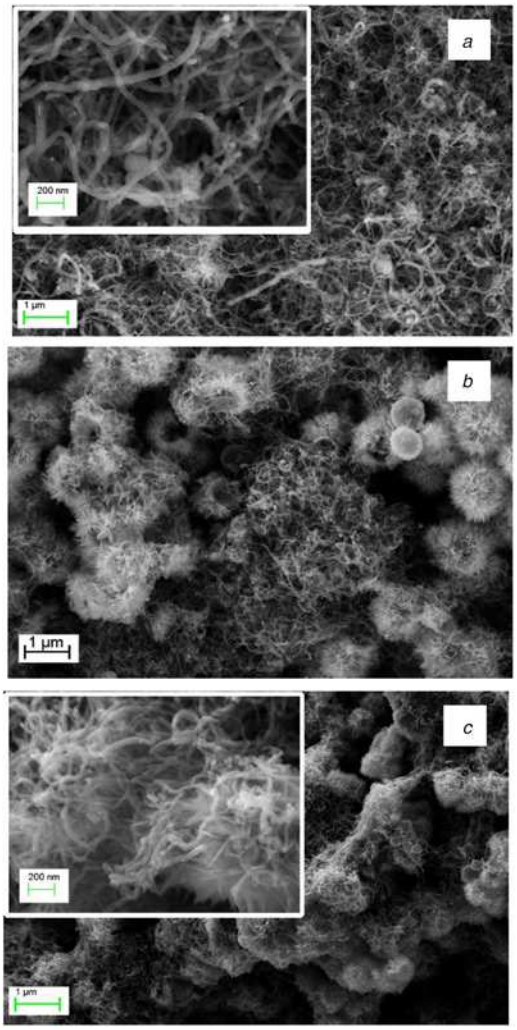

Fig. 1 *Scanning electron micrographs of*
a MWCNTs
b Hierarchical nanocomposite AH/MWCNTs
c Hierarchical nanocomposite AH/IH/MWCNTs

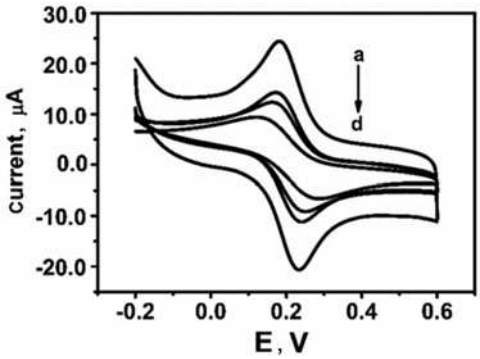

Fig. 2 *CVs of*
a bare GCE
b MWCNTs-GCE
c AH/MWCNTs-GCE
d AH/IH/MWCNTs –GCE in 1 mM $[Fe(CN)_6]^{3+}$ containing 0.1 M KCl

3.3. Electrochemical characterisation of NADH at different modified electrodes: Fig. 3 shows the electrochemical response of NADH at different electrodes in 0.1 M PBS (pH 7.4) without and with 50 µM NADH, respectively. When the potential of the GCE is scanned from 0 to 1 V, a weak and distorted irreversible anodic

doi: 10.1049/mnl.2020.0073

peak can be found at around 0.7 V due to a poisoning effect (Fig. 3*A*) [26]. The oxidation peak potential shifted to 0.40 V and the peak current increased by 80% for MWCNTs–GCE, suggesting enhanced catalytic oxidation of NADH on this electrode (Fig. 3*B* curve a). When the GCE surface was modified by AH/MWCNTs, the peak potential has an obvious decrease in comparison with MWCNTs–GCE [27]. Among all these electrodes, the highest peak current observed was for AH/IH/MWCNTs–GCE, and the lowest oxidation potential of NADH was about 0.15 V (Fig. 3*B* curve c). These results demonstrate that AH/IH as an electron-exchanger could greatly accelerate the process of NADH catalytic oxidation [22]. Moreover, positively charged AH/IH has a high-specific surface area due to the hierarchical structure, which can be employed as an adsorbent to enrich NADH and to enhance the oxidation current.

To understand the reaction mechanism, NADH electrocatalytic oxidation on this modified electrode was further researched by CV at various scan rates. From Fig. 4*A* we can see, upon gradually increasing the scan rate from 10 to 200 mV/s, the peak current of NADH increases, and the oxidation potential shifts to more positive values. This fact is an indication of the system's irreversibility [28]. A good linear relationship was observed between the current and scan rate, which indicates that the electrochemical redox process was that of a surface-controlled process (Fig. 4*B*).

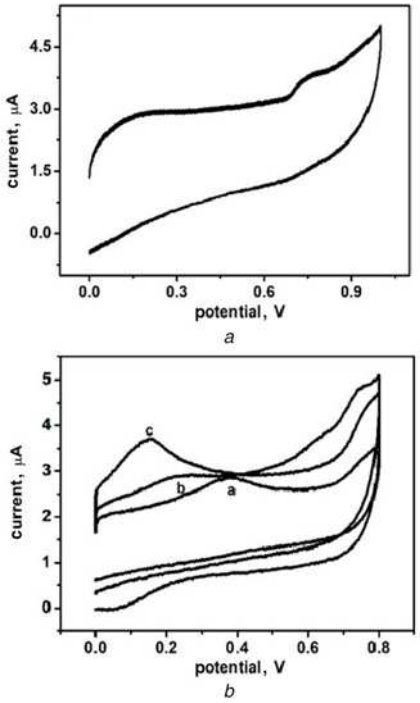

Fig. 3 *Cyclic voltammograms of different electrodes*
A Cyclic voltammograms of 0.1 mM NADH at bare GCE
B Cyclic voltammograms of 0.1 mM NADH at (a) MWCNTs-GCE, (b) AH/MWCNTs-GCE, and (c) AH/IH/MWCNTs-GCE

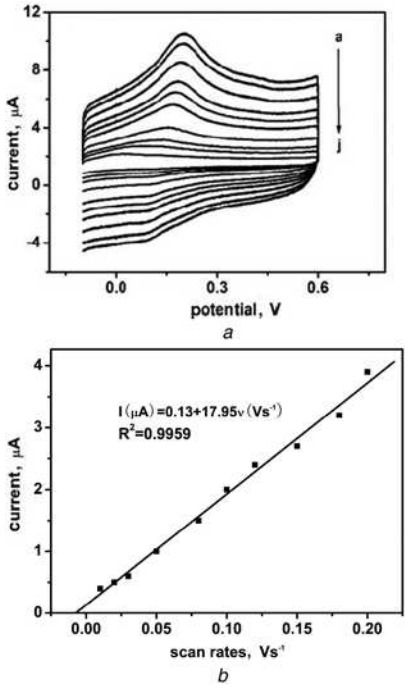

Fig. 4 *Cyclic voltammograms of the proposed electrode at various scan rates*
A Cyclic voltammograms at 0.01, 0.02, 0.03, 0.05, 0.08, 0.1, 0.12, 0.15, 0.18, and 0.2 V s^{-1} on the AH/IH/MWCNTs–GCE in the presence of 0.1 mM NADH, 0.1 M PBS (pH 7.4)
B Anodic peak current of NADH versus scan rate

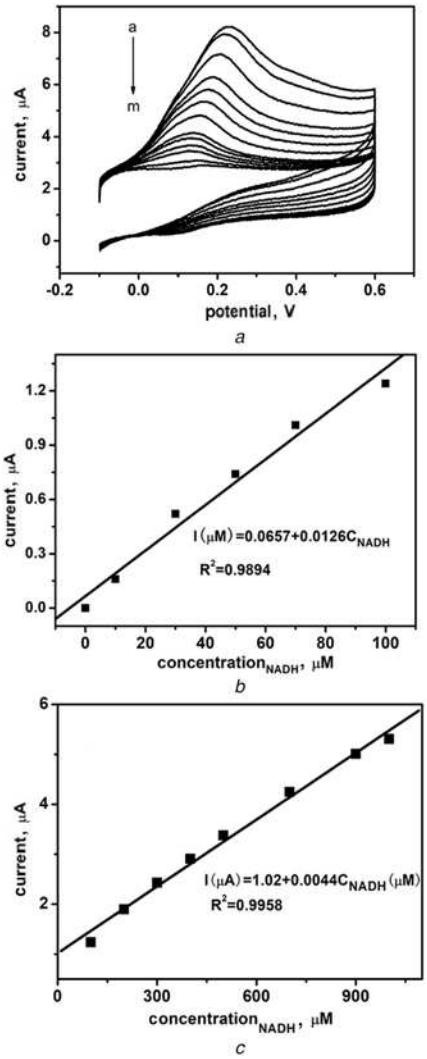

Fig. 5 *The response of the proposed electrode for NADH*
A Cyclic voltammograms of the AH/IH/MWCNTs–GCE in PBS as a function of NADH concentration: (a)–(m) 0, 10, 30, 50, 70, 100, 200, 300, 400, 500, 700, 900, and 1000 μM
B Calibration curves of the NADH concentrations (0, 10, 30, 50, 70, and 100 μM) versus the anodic peak currents
C Calibration curves of the NADH concentrations (100, 200, 300, 400, 500, 700, 900, and 1000 μM versus the anodic peak currents

3.4. Determination of NADH by the modified electrode sensor: To assess the response of AH/IH/MWCNTs–GCE for NADH, CV detection was carried out as a function of NADH concentration in 0.1 M PBS. The peak current increased with the NADH concentration, as shown in Fig. 5*A*. Anodic current consists of the anodic currents from adsorbed and diffusion species of NADH and their contribution to the anodic current varies with the concentration of NADH, so there are two calibration graphs from 10 to 1000 μM (Figs. 5*B* and *C*). The response of the proposed sensor had two linear concentration ranges: one from 10 to 100 μM, with a linear regression equation of $I(\mu A) = -0.065 - 0.013C_{NADH}$ (μM) ($R_2 = 0.9894$), and sensitivity of 0.013 μA/μM; and another from 100 to 1000 μM, with a linear regression equation of $I(\mu A) = -1.02 - 0.0044C_{NADH}$ (μM) ($R_2 = 0.9958$), and sensitivity of 0.004 μA/μM. The detection limit was determined to be 5 μM. It can be inferred that the AH/IH/MWCNTs nanomaterial possess good properties and fits for the construction of NADH detection systems.

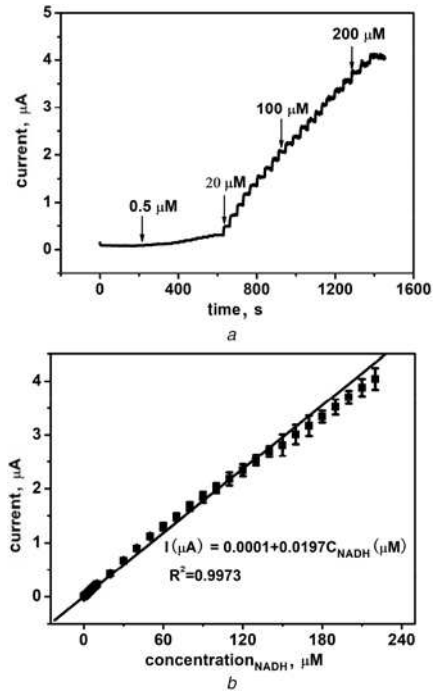

Fig. 6 *Amperometric detection of NADH on the proposed electrode*
a Amperometric *i–t* curve using AH/IH/MWCNTs-GCE in 0.1 M PBS with varying concentration of NADH at 0.15 V
b Calibration plot for AH/IH/MWCNTs-GCE

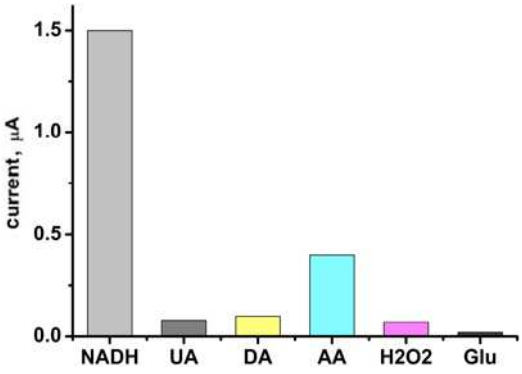

Fig. 7 *Interference data for AH/IH/MWCNTs–GCE for oxidation of NADH*

3.5. Amperometric detection of NADH on the proposed electrode: To reduce background current and improve electrode performance [21], amperometric detection of NADH on the AH/IH/MWCNTs–GCE was performed at a potential of 0.15 V in stirred PBS using current–time (*I–t*) methods. As presented in Fig. 6*a*, it is very fast for the amperometric response to the successive addition of NADH. The current increased to 95% of the steady-state is reached within 3 s. The calibration curve indicated that it has a linear response to NADH in the range of 0.5–220 μM with a detection limit of 0.30 μM (signal-to-noise ratio $S/N = 3$) (Fig. 6*b*). The sensitivity of the present sensor was 0.02 μA/μM. The relative standard deviation for 50 μM NADH was 4.3% (for six detection), suggesting that the electrode has high repeatability. To evaluate the selectivity of the electrode, the influence of interference for NADH was also carefully investigated. The results of this evaluation were displayed in Fig. 7. The amperometric measurement was performed by the addition of NADH (50 μM) and the interfering compounds (50 μM) in 0.1 M PBS. No obvious current response was observed in the presence of urea, hydrogen peroxide (H_2O_2), glucose (Glu), dopamine but a big oxidation current of ascorbic acid (AA) was observed. These results demonstrated that this electrode had good selectivity for the determination of NADH. The analytical performance of the present electrode has been compared to other NADH sensors reported in recent years in Table 1.

The proposed modified electrode was used as a novel dehydrogenase-based biosensing platform by incorporating enzyme into the AH/IH/MWCNTs film. Owing to the strong electrostatic among AH/IH, MWCNTs, and enzyme, a model enzyme ADH can be firmly immobilised in this multilayer structure. The amperometric response was recorded at 0.15 V with successive additions of ethanol in a stirred 0.1 M PBS (pH 7.4) containing 3.0 mM NAD^+. As shown in Fig. 8, there is an increase in the current response upon the addition of ethanol, and a stable response is obtained within 3 s. This is due to the formation and subsequent oxidation of NADH during the enzymatic catalysis. The current response increased linearly with

Table 1 Response characteristics of different NADH sensors

Electrode/nanomaterial	Epa (V) versus Ag/AgCl	Limit of detection (LOD), μM	Linear range, mM	Ref
Screen printed electrodes (SPE)/MWCNT microwave oxidised	0.27	1	4.0×10^{-3}–3.5×10^{-2}	[29]
GCE/MWCNT/poly-ferulic acid (FA)	0.20	17.73	5.91×10^{-2}–1.56	[20]
Reduced graphene oxide (rGO)/poly(methylene blue)/AgNPs paper	0.535	0.072	2.5×10^{-4}–0.4	[14]
Fe_3O_4/(Ionic liquid crystals (ILC)-CNTs)/GCE	0.25	0.0346	5×10^{-3}–0.7	[17]
Fe_3O_4NPs/rGO/GCE	0.05	0.4	2×10^{-3}–1.5×10^{-2}	[22]
Pt/Fe_3O_4 /rGO/GCE	0.48	0.005	3×10^{-5}–1.5×10^{-3}	[21]
Phthalic diglycol diacrylate (PDDA)-rGO/GCE	0.24	0.034	1×10^{-4}–2.9	[30]
GCE/Au-AgNPs/P(L-cysteine)/electrochemically reduced graphene oxide (ERGO)	0.35	0.009	8.2×10^{-5}–7.3×10^{-2} 7.3×10^{-2}–1.05	[31]
AH/IH/MWCNTs	0.10	0.15	5×10^{-4}–0.22	this work

doi: 10.1049/mnl.2020.0073

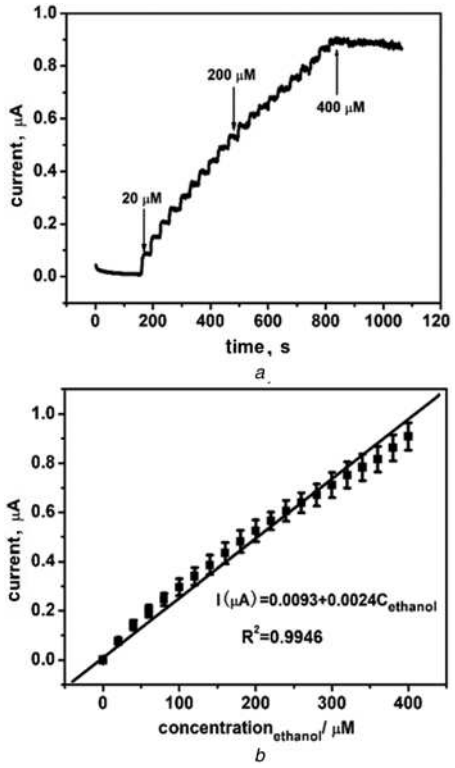

Fig. 8 *Amperometric detection of ethanol on the ADH/AH/IH/MWCNTs-GCE*
a Amperometric *i–t* curve using ADH/AH/IH/MWCNTs-GCE in the presence of 3.0 mM NAD^+ in 0.1 M PBS (pH 7.4) with varying concentrations of ethanol at 0.15 V
b Calibration plot for AH/IH/MWCNTs-GCE

the ethanol concentration in the range of 20–400 μM, with a linear regression equation of $I(\mu A) = -0.0093 + 0.0097\ C_{Ethanol}\,(\mu M)$ ($R^2 = 0.9946$), and sensitivity of 9.7 μA/mM. The limit of detection was calculated as 5 μM ($S/N = 3$), which is comparable to or better than those obtained by other ADH amperometric biosensors based on nanocomposite [32–35].

4. Conclusions: In this study, we synthesised AH/IH/MWCNTs' nanocomposites with which we modified GCEs. AH is uniquely advantageous to serve as catalyst support to uniformly anchor $Fe(OH)_3$ colloid nanoparticles and agglomeration is no longer an issue. The electrocatalytic properties of the obtained material towards the oxidation of NADH were investigated thoroughly. Compared with the electrode of MWCNTs–GCE, the overpotential for NADH oxidation was obviously decreased for the AH/IH/MWCNTs-modified electrode, and the current response was significantly improved. Moreover, AH/IH/MWCNTs–GCE was utilised for the determination of ethanol by exploiting the reaction of ethanol with NAD^+ and ADH, which forms NADH. However, this method has low stability and AA can interfere with the determination of NADH. Efforts to improve the reproducibility and stability through current measurements are currently in progress in this laboratory.

5. Acknowledgments: This work was financially supported by the Natural Science Foundation of Shandong Province (ZR2016CB25), the Scientific Research Foundation of the Higher Education Institutions of Shandong Province (J16LE56) and Project supported by the National Natural Science Foundation of China (61801274).

6 References

[1] Jaegfeldt H., Kuwana T., Johansson G.: 'Electrochemical stability of catechols with a pyrene side chain strongly adsorbed on graphite electrodes for catalytic oxidation of dihydronicotinamide adenine dinucleotide', *J. Am. Chem. Soc.*, 1983, **105**, pp. 1805–1814
[2] Xie W., Xu A., Yeung E.S.: 'Determination of NAD^+ and NADH in a single cell under hydrogen peroxide stress by capillary electrophoresis', *Anal. Chem.*, 2009, **81**, pp. 1280–1284
[3] Lin S.J., Guarente L.: 'Nicotinamide adenine dinucleotide, a metabolic regulator of transcription, longevity and disease', *Curr. Opin. Cell Biol.*, 2003, **15**, pp. 241–246
[4] Zhao Y.Z., Lin J., Hu Q.X., *ET AL.*: 'Genetically encoded fluorescent sensors for intracellular NADH detection', *Cell Metab.*, 2011, **14**, pp. 555–566
[5] Kaur R., Sidhu J.S., Singh N., *ET AL.*: 'Cystamine-cobalt complex based fluorescent sensor for detection of NADH and cancer cell imaging', *Sens. Actuators B, Chem.*, 2019, **293**, pp. 144–150
[6] Riedel M., Hölzel S., Hille P., *ET AL.*: 'Ingan/Gan nanowires as a new platform for photoelectrochemical sensors-detection of NADH', *Biosens. Bioelectron.*, 2017, **94**, pp. 209–304
[7] Warren S., Munteanu G., Rathod D., *ET AL.*: 'Scanning electrochemical microscopy imaging of poly(3,4-ethylendioxythiophene)/thionine electrodes for lactate detection via NADH electrocatalysis', *Biosens. Bioelectron.*, 2019, **137**, pp. 15–24
[8] Li X.Y., Kan X.W.: 'A boronic acid carbon nanodots/poly(thionine) sensing platform for the accurate and reliable detection of NADH', *Bioelectrochemistry*, 2019, **130**, p. 107344(1–7)
[9] Kang J., Shin J., Yang H.: 'Rapid and sensitive detection of NADH and lactate dehydrogenase using thermostable DT-diaphorase immobilized on electrode', *Electroanalysis*, 2018, **30**, pp. 1357–1362
[10] Aneesh K., Raovusa C.S., Berchmans S.: 'Enhanced peroxidase-like activity of $CuWO_4$ nanoparticles for the detection of NADH and hydrogen peroxide', *Sens. Actuators B, Chem.*, 2017, **253**, pp. 723–730
[11] Blaedel W.J., Jenkins R.A.: 'Study of the electrochemical oxidation of reduced nicotinamide adenine dinucleotide', *Anal. Chem.*, 1975, **47**, pp. 1337–1343
[12] Wang J., Angenes L., Martinez T.: 'Scanning tunneling microscopic probing of surface fouling during the oxidation of nicotinamide coenzymes', *Bioelectrochem. Bioenerg.*, 1992, **29**, pp. 215–221
[13] Omar F.S., Duraisamy N., Ramesh K., *ET AL.*: 'Conducting polymer and its composite materials based electrochemical sensor for nicotinamide adenine dinucleotide (NADH)', *Biosens. Bioelectron.*, 2016, **79**, pp. 763–775
[14] Topçu E., Dagci K., Alanyalioglu M.: 'Free-standing graphene/poly (methylene blue)/AgNPs composite paper for electrochemical sensing of NADH', *Electroanalysis*, 2016, **28**, pp. 2058–2069
[15] Han S.Y., Du T.Y., Jiang H., *ET AL.*: 'Synergistic effect of pyrroloquinoline quinone and graphene nano-interface for facile fabrication of sensitive NADH biosensor', *Biosens. Bioelectron.*, 2017, **89**, pp. 422–429
[16] Musameh M., Wang J., Merkoci A., *ET AL.*: 'Low-potential stable NADH detection at carbon-nanotube-modified glassy carbon electrodes', *Electrochem. Commun.*, 2002, **4**, pp. 743–746
[17] Atta N.F., Gawad S.A.A., EI-Ads E.H., *ET AL.*: 'A new strategy for NADH sensing using ionic liquid crystals-carbon nanotubes/nano-magnetite composite platform', *Sens. Actuators B, Chem.*, 2017, **251**, pp. 65–73
[18] Li J., Sun Q.Q., Mao Y.J., *ET AL.*: 'Sensitive and low-potential detection of NADH based on boronic acid functionalized multi-walled carbon nanotubes coupling with an electrocatalysis', *J. Electroanal. Chem.*, 2017, **794**, pp. 1–7
[19] Li Y.W., Chen Y., Ma Y.H., *ET AL.*: 'Recent advances in the dehydrogenase biosensors based on carbon nanotube modified electrodes', *Chin. J. Anal. Chem.*, 2014, **42**, pp. 759–765
[20] Silva L.V.D.C., Lopes B., Silva W.C.D., *ET AL.*: 'Electropolymerization of ferulic acid on multi-walled carbon nanotubes modified glassy carbon electrode as a versatile platform for NADH, dopamine and epinephrine separate detection', *Microchem. J.*, 2017, **133**, pp. 460–467
[21] Roushani M., Hoseini S.J., Azadpour M., *ET AL.*: 'Electrocatalytic oxidation behavior of NADH at Pt/Fe_3O_4/reduced-graphene oxide nanohybrids modified glassy carbon electrode and its determination', *Mater. Sci. Eng. C.*, 2016, **67**, pp. 237–246
[22] Teymourian H., Salimi A., Hallaj R.: 'Low potential detection of NADH based on Fe_3O_4 nanoparticles/multiwalled carbon nanotubes composite: fabrication of integrated dehydrogenase-based lactate biosensor', *Biosens. Bioelectron.*, 2012, **33**, pp. 60–68
[23] Zhang Y.X., Zhou X.B., Liu Z.L., *ET AL.*: 'Monodispersed hierarchical γ-AlOOH/$Fe(OH)_3$ micro/nanoflowers for efficient removal of heavy metal ions from water', *RSC Adv.*, 2016, **6**, pp. 6695–6700

[24] Zhang Y.X., Ye Y.J., Zhou X.B., *ET AL.*: 'Monodispersed hollow aluminosilica microsphere@hierarchical γ-AlOOH deposited with or without $Fe(OH)_3$ nanoparticles for efficient adsorption of organic pollutants', *J. Mater. Chem. A.*, 2016, **4**, pp. 838–846
[25] Velasco J.G.: 'Determination of standard rate constants for electrochemical irreversible processes from linear sweep voltammograms', *Electroanalysis*, 1997, **9**, pp. 880–882
[26] Govindhan M., Amiri M., Chen A.: 'Au nanoparticle/graphene nanocomposite as a platform for the sensitive detection of NADH in human urine', *Biosens. Bioelectron.*, 2015, **66**, pp. 474–480
[27] Mekawy M.M., Hassan R.Y.A., Ramnani P., *ET AL.*: 'Electrochemical detection of dihydronicotinamide adenine dinucleotide using Al_2O_3-GO nanocomposite modified electrode', *Arab. J. Chem.*, 2018, **11**, pp. 942–949
[28] Rajaram R., Anandhakumar S., Mathiyarasu J.: 'Electrocatalytic oxidation of NADH at low overpotential using nanoporous poly (3,4-ethylenedioxythiophene) modified glassy carbon electrode', *J. Electroanal. Chem.*, 2015, **746**, pp. 75–81
[29] Blandón-Naranjo L., Pelle F.D., Vázquez M.V., *ET AL.*: 'Electrochemical behaviour of microwave-assisted oxidized MWCNTs based disposable electrodes: proposal of a NADH electrochemical sensor', *Electroanalysis*, 2018, **30**, pp. 509–516
[30] Lu J.J., Liu Y.L., Liu X.H., *ET AL.*: 'Construction of a highly sensitive NADH sensing platform based on PDDA–rGO nanocomposite modified electrode', *Ionics*, 2016, **22**, pp. 2225–2233
[31] Tig G.A.: 'Highly sensitive amperornetric biosensor for determination of NADH and ethanol based on Au–Ag nanoparticles/poly(L-cysteine)/reduced graphene oxide nanocomposite', *Talanta*, 2017, **175**, pp. 382–389
[32] Barhoumi L., Istrate O.M., Rotariu L., *ET AL.*: 'Amperometric determination of ethanol using a novel nanobiocomposite', *Anal. Lett.*, 2017, **51**, pp. 323–335
[33] Bilgi M., Sahin E.M., Ayranci E.: 'Sensor and biosensor application of a new redox mediator: rosmarinic acid modified screen-printed carbon electrode for electrochemical determination of NADH and ethanol', *J. Electroanal. Chem.*, 2018, **813**, pp. 67–74
[34] Gutierrez F., Rubianes M.D., Rivas G.A.: 'Dispersion of multi-wall carbon nanotubes in glucose oxidase: characterization and analytical applications for glucose biosensing', *Sens. Actuators B, Chem.*, 2012, **161**, pp. 191–197
[35] Teymourian H., Salimi A., Khezrian S.: 'Fe_3o_4 magnetic nanoparticles/reduced graphene oxide nanosheets as a novel electrochemical and bioeletrochemical sensing platform', *Biosens. Bioelectron.*, 2013, **49**, pp. 1–8

doi: 10.1049/mnl.2020.0073